Talanta 114 (2013) 204–210

Contents lists available at ScienceDirect

Talanta

journal homepage: www.elsevier.com/locate/talanta

Probing trace Hg^{2+} in a microfluidic chip coupled with in situ near-infrared fluorescence detection

Jiaqin Wang, Hui Chen, Peng Zhang, Zhengyong Zhang, Song Zhang, Jilie Kong *

Department of Chemistry, CAM & IBS, Fudan University, Shanghai, PR China

ARTICLE INFO

Article history:
Received 30 November 2012
Received in revised form
25 March 2013
Accepted 28 March 2013
Available online 6 April 2013

Keywords:
Near-infrared (NIR) fluorescence
Microfluidic chips
Single-walled carbon nanotubes (SWNTs)

ABSTRACT

A novel microfluidic chip coupled with near-infrared (NIR) fluorescence detection set-up was established for specific analysis of trace Hg^{2+}. Based on the NIR fluorescence changes caused by Hg^{2+}-induced dissolution and aggregation of label-free single-strand DNA (ssDNA) wrapped single-walled carbon nanotubes (SWNTs), Hg^{2+} in aqueous solution were detected sensitively and specifically in the microfluidic chips system. Due to the small device dimension effect as well as the high efficiency of microfluidic chips, the reagent volume reduced from 500 μL to 9 μL and the minimum reaction time reaching the plateau was shortened from 60 min to 30 min, while the detection limit for Hg^{2+} decreased from 10.5 nM to 1.5 nM, compared with that of measured in regular Eppendorf tube. The idea of detecting NIR fluorescence spectra in microfluidic systems opens new avenues to optical analysis and bioassays in probing trace species.

1. Introduction

Single-walled carbon nanotubes (SWNTs) have gained a lot of interest in electronics, optics, chemistry, biosensing [1] and drug delivery fields [2,3], owing to their unique structural, mechanical, electrical and biocompatible properties. Recently, individual semiconductive SWNTs have been demonstrated to emit fluorescence in the near-infrared (NIR) range within the "biological window" (700–1300 nm) where the autofluorescence background and absorption of tissue and biological media are minimized [4]. Single-strand DNA (ssDNA) has been ably employed to wrap SWNTs and obtain its NIR fluorescence because ssDNA interact noncovalently with SWNT through π-stacking between the bases of the ssDNA and the atomic structures on the sidewall of SWNTs [5]. Therefore, both the biological recognition ability of ssDNA and NIR fluorescence of SWNT can be remained intact, which has been employed in the sorting of SWNTs and detection of nucleic acids and proteins [6–8]. However, most of assays need large volume of DNA wrapped SWNTs solutions and long biochemical reaction time, which limits their widespread application in bioanalysis and environmental surveillance.

Microfluidic chips system, also called lab-on-a-chip, has developed rapidly in the past ten years. Well-known for their advantages such as small volume of sample, short reaction time and high throughput, microfluidic chips systems provide attractive vistas in disease diagnose [9], cell biology [10] and drug screening [11,12]. Among many kinds of detection methods in microfluidic chips, laser induced fluorescence detection method plays an important role in bioassay. However, so far as we known, no study has been conducted using NIR fluorescence detection in microfluidic chip system. In order to integrate the both merits (such as low background, long penetration length) of NIR method in microfluidic chip and solve the neck-bottle problems based on NIR fluorescence of DNA wrapped SWNT, we merged these two concepts and evaluated the improved performance.

To investigate the efficiency of NIR-on-chip, we take mercury ion (Hg^{2+}) as the target analyte, which is a widespread pollutant with distinct toxicological profiles and may cause brain damage as well as other chronic diseases [13]. According to National Secondary Drinking Water Regulations (NSDWR, USA), the concentration of Hg^{2+} in drinking water must be below 0.002 mg/L (=10 nM) [14]. The particular formation of thymine–Hg^{2+}–thymine (T–Hg^{2+}–T) mismatches between Hg^{2+} and ssDNA has been well studied and used in Hg^{2+} detection recently, for it has high selectivity for Hg^{2+} against other metal ions. However, while using 6-carboxyfluorescein (FAM) labeled T-rich ssDNA wrapped SWNTs in Hg^{2+} detection [15,16] or integrating T–Hg^{2+}–T complexes with gold nanoparticles (AuNPs) [17,18], the detection limit can hardly satisfy 10 nM in optical analysis. Therefore, developing an approach much more efficient for detecting trace Hg^{2+} with ultra-high sensitivity is of considerable significance. On the other hand, the NIR fluorescence of the SWNTs can be quenched when individually dispersed SWNTs aggregate into bundles [4], which has been applied in the assay of biomolecules such as glucose and thrombin

* Corresponding author. Tel.: +86 21 65642405; fax: +86 21 65641740.
E-mail address: jlkong@fudan.edu.cn (J. Kong).

0039-9140/$ - see front matter © 2013 Elsevier B.V. All rights reserved.
http://dx.doi.org/10.1016/j.talanta.2013.03.079

[8,19]. To the best of our knowledge, there is no published paper involving employing the concept of reversible dissolution and aggregation of label-free ssDNA/SWNTs for Hg^{2+} detection.

Therefore, in this study, we herein present a novel NIR fluorescence detection method in microfluidic chips system based on Hg^{2+}-induced aggregation of label-free ssDNA wrapped SWNTs. This assay is proved to be more sensitive and fast as compared with the measurement in Eppendorf tube and is amenable to other optical analysis applications.

2. Experimental section

2.1. Materials

The polyacrylamide gel electrophoresis (PAGE) purified mercury-specific ssDNA (5′–TTCTTTCCCCTTTGTT-3′, named as d16) was synthesized by Shanghai Sangon Biotechnology Co. Ltd. (Shanghai, China). The as-grown SWNTs (HiPCo) were purchased from Carbon Nanotechnologies, Inc. (Houston, TX, USA). Poly(dimethylsiloxane) (PDMS, Sylgard 184) was obtained from Dow Corning (Midland, MI, USA). 1H,1H,2H,2H-Perfluorodecyltriethoxysilane (97%) was purchased from Alfa-Aesar. Standard solution with Hg^{2+} concentration at 50 mg/L (= 250 μM) was purchased from National Institute of Standards and Technology (NIST). Unless indicated specifically, all the other reagents were bought from Sinopharm Chemical Reagent Co. Ltd. (Shanghai, China). Metal ion solutions were prepared from chloride salts. Tris-HCl buffer (10 mM, pH=7.4) prepared in Milli-Q water was used all through the experiments. Environmental water sample was taken from a nearby river in Fudan University.

2.2. Characterization instruments

UV–visible absorbance spectra were recorded on a Shimadzu UV-3150 UV–vis–NIR spectrophotometer at room temperature using a 500 μL quartz cuvette with optical path at 1 cm. AFM images were imaged with Nanoscope IV (Veeco, USA) atomic force microscope operated in tapping mode. A typical AFM sample was prepared by pre-treat a piece of freshly cleaved mica surface with 10 μL 1 M $MgCl_2$ aqueous solution for 1 min, washing four times with water to remove salts, and then spotting the drop of 15 μL sample solution onto the mica surface. After culturing for 10 min, the mica piece was rinsed with water and blown to dry by compressed air. All CD spectra were recorded on a Jasco-715 spectropolarimeter (Tokyo, Japan) equipped with a programmable temperature controlled water bath. The optical chamber of CD spectrometer was deoxygenated with dry purified nitrogen (99.99%) for 45 min before use and kept the nitrogen atmosphere during experiments. The sample injections to the microfluidic system were carried out by LongerPump LSP02-1B and Cole-Parmer 789000 peristaltic pumps.

2.3. Preparation of d16/SWNTs solution [8]

In a typical method, the as-grown SWNTs (HiPCo) (0.5 mg), mixed with d16 (0.2 mg) in Tris-HCl buffer, were sonicated for 4 h (the temperature was controlled lower than 30 degree by ice-water bath) to give a homogeneous black solution. Then the colloid solution was centrifuged at 14,000 rpm for 2 h to discard the pellet comprising of impurities, aggregates, and bundles of SWNTs at the bottom of the centrifuge tube. To remove the free DNA, the supernatant was collected and underwent an additional centrifugation round at 5000 rpm with a 30 K molecular weight cut-off (MWCO) membrane for 15 min. And then the Tris-HCl buffer solution was added to re-suspend the d16/SWNT. The prepared homogenous d16/SWNTs solution used for the following quantitative detections and selectivity studies contains about 8 mg/L SWNTs and about 14 nM d16 (≈8.43×10^{15} copies/L).

2.4. Fabrication of the microfluidic chips system

The master of chip with desired patterns was fabricated by mechanical microfabrication [9]. In brief, PDMS was casted onto the plexiglass engraved with a Y shape microchannel and then put in oven at 80 °C for 2 h as a master. After passivation, the master was coated by PDMS and baked to get a patterned PDMS chip. Then the PDMS chip was bonded to a microscope slide using oxygen plasma cleaner.

2.5. Confirmation of chip dimensions and sample injection rates

A PDMS replica was produced by molding as described previously. We evaluated the mix efficiency in diversity of microchannels with width ranging from 600 to 1500 μm, height ranging from 240 to 600 μm. The final dimensions we choose for whole microfluidic chip are 1.5 cm (width) × 3 cm (length) while dimensions of the microchannel of this device are 800 μm (width) × 450 μm (height). (As shown in Fig. 1a)

To retain the high NIR fluorescence of d16/SWNT solution, we set injection rates of the two liquid reactors as 108 μL/h (d16/SWNTs solution):12 μL/h (liquid sample with Hg^{2+}) using peristaltic pumps. The injection time was modulated to 4 min to ensure mixing the two reactors completely while the total injection volume was 9 μL. As shown in Fig. 1b, we use Methylene blue (blue) and p-nitrophenol (yellow) solutions to represent d16/SWNTs solution and Hg^{2+} contained liquid sample, respectively. The mixture turned to homogenous green near the outlet of microchannel through commixing in the middle part, whereas the boundary of blue and yellow liquid remained distinct at the foreside. This mix efficiency obviously illustrated that d16/SWNTs solution would totally mix and react with Hg^{2+} after injection at the detection point.

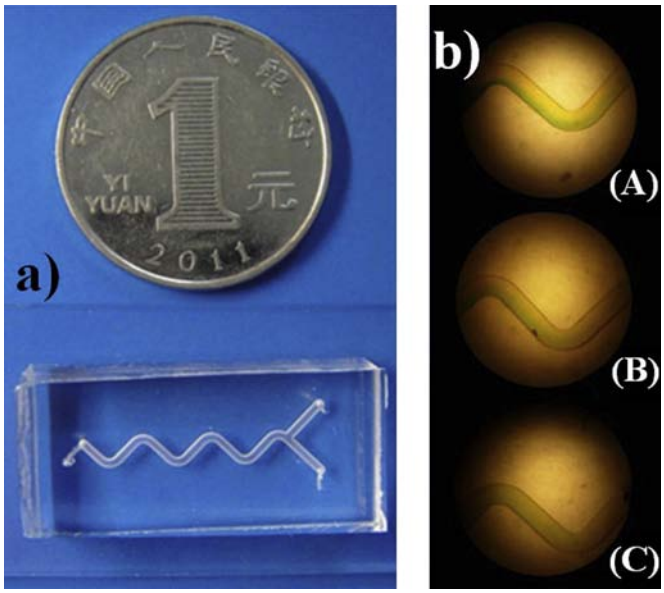

Fig. 1. (a) Real photo of the microfluidic device. (b) Microscope photos of mixture containing methylene blue (blue) and p-nitrophenol (yellow) solutions in the part of microchannel (A) close to the inlets; (B) in the middle; (C) near the outlet. (For interpretation of the references to color in this figure legend, the reader is referred to the web version of this article.)

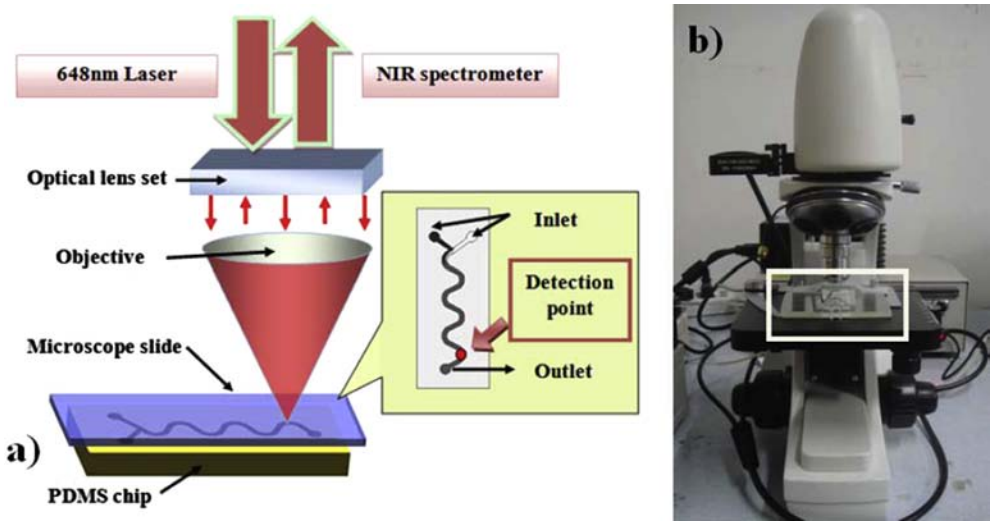

Fig. 2. (a) Basic components of home-assembled NIR-on-chip detection set-up and the shape of microchannel. Ensemble measurement setup: focus on the detection point of microfluidic chip, SWNT solution is excited by a 648 nm laser in a custom microscope setup, then the resulting emission spectra are recorded and analyzed. (b) Real photo of the detection equipment, microfluidic chip was placed on the sample stage within the white rectangular part.

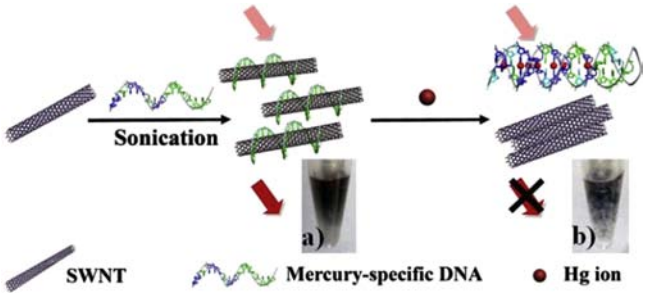

Scheme 1. Principle of Hg^{2+} detection based on the NIR fluorescence changes caused by dissolution and aggregation of SWNT. Inset: real photos of (a) dispersed homogeneous black d16/SWNT solution and (b) aggregation of SWNTs when final Hg^{2+} concentration was at 500 nM in Eppendorf tubes.

2.6. Operation of NIR-on-chip detection set-up

Fig. 2 shows the schemes and photographs of basic components for this NIR-on-chip detection method. The microfluidic device is made by adhering the channel contained PDMS chip with microscope slide. Since PDMS has a slight absorption in NIR field, microscope slides are put ascendingly at the same side of laser input in the detection for their equal thickness and optical transparent property. The chip comprised a zigzag reaction channel of 800 μm width and two inlet channels, each supplied with one liquid reactor by different pumps. Focus on the detection point near the outlet of microchannel, SWNT solution would fully mix and react with Hg^{2+} and NIR spectrum of the mixture could then be recorded. The near infrared photoluminescence of the SWNTs solution was illuminated with 648 nm laser and the fluorescence signal was collected with a BTC261E-512-element InGaAs spectrometer (BWTEK, USA).

3. Results and discussion

3.1. Principle of Hg^{2+} induced aggregation of d16/SWNT

The principle for probing Hg^{2+} was illustrated in Scheme 1, which is based on the NIR fluorescence changes of ssDNA wrapped SWNTs triggered by Hg^{2+}. When Hg^{2+} specific DNA (d16) has been sonicated with SWNTs for certain time, SWNTs shows individually dispersed states and emits strong NIR fluorescence. Upon addition of Hg^{2+}, strong and specific reactions between d16 ssDNA and Hg^{2+} gives rise to the formation of hairpin structure, via thymine–Hg^{2+}–thymine (T–Hg^{2+}–T) mismatches and results in the detaching of d16 ssDNA from the sidewall of SWNTs. Without the π–π interaction between ssDNA and SWNTs, the aggregation of SWNTs occurs and hence quenches the NIR fluorescence emission. Therefore, the intensity of NIR fluorescence was correlated with the recognition of Hg^{2+}. Although the fluorescence of SWNTs can be also quenched by Hg^{2+}, the minimum concentration of Hg^{2+} for quenching needs to be above 1 mM [20]. Thus the idea of bringing trace Hg^{2+} detection at nanomolar level into NIR field using the fluorescence of SWNT is feasible. The aggregation of SWNTs from dispersed homogeneous black solution was also seen by naked eyes in Eppendorf tubes when final Hg^{2+} concentration was at 500 nM. (inset of Scheme 1)

To characterize the interaction between the d16/SWNTs and Hg^{2+}, homogeneous black d16/SWNTs solutions with different concentration of Hg^{2+} were monitored using the circular dichroism (CD) spectrophotometer. As shown in Fig. 3a, the d16 on SWNT exhibited negative and positive peaks around 232 and 330 nm, respectively. Coordinated with the concentration of Hg^{2+} from 0 to 250 nM, the peak intensities at 330 nm as well as 232 nm both gradually decreased, indicating the tightness of d16 wrapping around SWNTs became loose. Formation of double helical T–Hg^{2+}–T base mismatched pairs ($K_b \approx 3.98 \times 10^6$ L mol^{-1}) [21] which weakened the interaction between d16 ssDNA and SWNTs, led to parts or all of d16 molecules peel off from the sidewalls of SWNTs. Similar decreases of positive and negative peaks intensities appeared in CD spectrum of free d16 solution with increased Hg^{2+} concentration in Fig. 3b. Compared with CD spectra of d16/SWNTs in Fig. 3a, the negative band of the free d16 DNA at about 248 nm became a little red-shifted while the positive band at about 285 nm showed rather blue-shifted. These changes of ellipticity about linear structure DNA were probably resulted from the interaction between bases and sidewalls of SWNTs.

To demonstrate the mercury-induced aggregation and dissolution state of SWNT, the d16/SWNT solution was characterized using UV–vis-NIR absorption spectroscopy (As shown in Fig. 4a). The sharp Van Hove peak of the direct band gap semiconducting SWNTs ranging from 800 to 1350 nm indicated that d16 wrapped SWNTs retained their electronic properties as sodium dodecylsulfate (SDS) dispersed SWNTs [4]. As seen in line B, the sample after

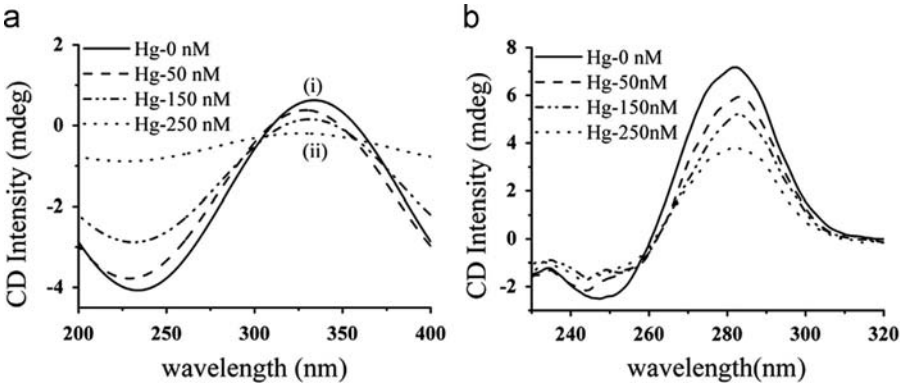

Fig. 3. (a) CD spectrum of d16/SWNT solution following incubation with Hg^{2+} in increasing concentrations, including 0 nM (i), 50 nM, 150 nM, 250 nM (ii), respectively. (b) CD spectrum of free d16 (100 μM) following incubation with Hg^{2+} in increasing concentrations, including 0 nM, 50 nM, 150 nM, 250 nM, respectively.

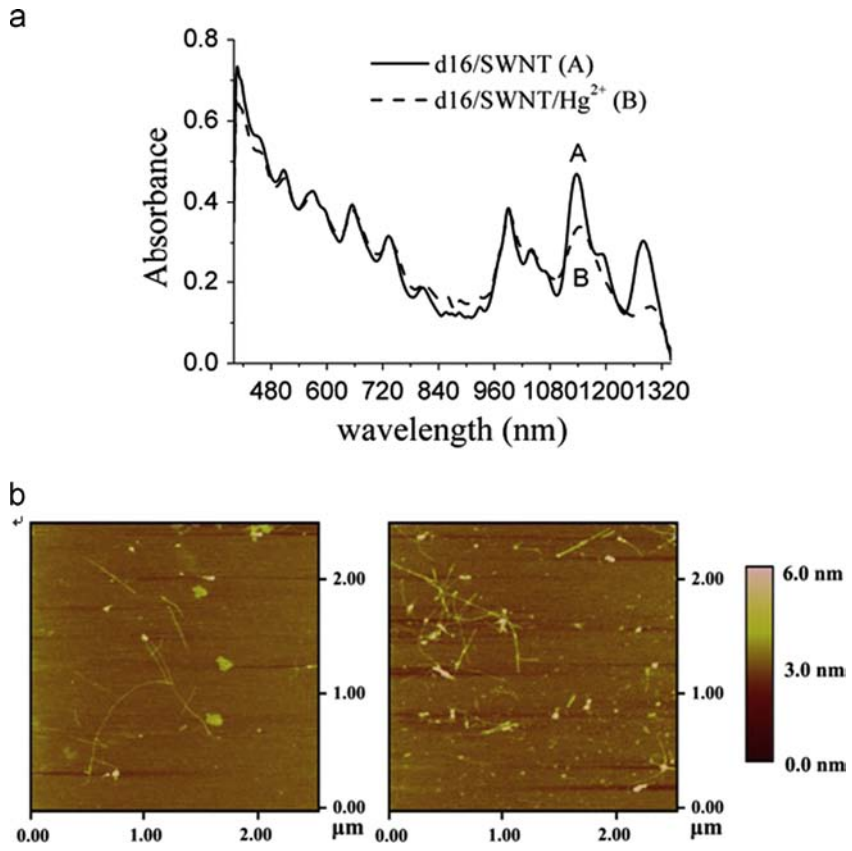

Fig. 4. (a) UV–vis-NIR absorption spectrum of the d16/SWNT solution before (A) and after (B) Hg^{2+} addition. (b) Tapping mode AFM height images of d16/SWNT without (left image) and with (right image) Hg^{2+} on fresh cleaved mica substrate pretreated with 1 M $MgCl_2$, scan bar at 2.5 μm.

adding Hg^{2+} shows markedly reduced absorption intensity especially in the near-infrared range from 1000 nm to 1320 nm, which resulted from the detachment of d16 on SWNTs. The individual semiconductive SWNTs tended to aggregate since their DNA-induced dispersion stability gradually lost.

Furthermore, the mercury-induced aggregation of SWNTs was also verified by atomic force microscopy (AFM) images in Fig. 4b. The SWNTs are well dispersed into mostly individual tubes in the absence of Hg^{2+} in the left image, with the height of each individual nanotube at about 4 nm. Through the π–stacking interaction, the d16 wrapped on the SWNT sidewall with the size of 1–2 nm made the height of a single d16/SWNT higher than the typical as-prepared SWNT (0.7–1.1 nm). In the presence of Hg^{2+}, d16/SWNTs aggregated into bundles in the right image because the electronic force between d16 and SWNTs was destroyed.

Taken together, these results successfully revealed that Hg^{2+} can trigger the aggregation of dispersed d16/SWNTs by forming T–Hg^{2+}–T complex and detaching d16 DNA from the surface of SWNTs. As far as we know, there are no reported works studying the above aggregation process using laser induced NIR fluorescence in aqua-dispersed ssDNA/SWNTs solution.

3.2. *Detection of Hg^{2+} in conventional Eppendorf tubes and microfluidic chips system*

The temperature effect were studied before the following experiments by collecting the NIR signals of two d16/SWNTs samples with exactly the same Hg^{2+} concentration and reaction time at different reaction temperatures. NIR curves were almost

coincident at 4 °C and 25 °C in both spectrograms which makes following measurements all perform at room temperature.

Inspired by aforementioned Hg^{2+} trigged aggregation of d16/SWNTs and aggregation induced quenching of SWNT NIR fluorescence [4,18], the NIR fluorescence properties of d16/SWNTs solution with different concentrations of the target Hg^{2+} were investigated in conventional Eppendorf tubes and microfluidic chips respectively for the sensitive, specific and fast assay of Hg^{2+}. It can be seen from Fig. 5 that NIR fluorescence emission spectra decreased gradually upon addition of Hg^{2+} ion, which verified the mercury triggered aggregation of individual SWNT. The fluorescence spectrum includes several peaks referring to different SWNT chiralities. The strongest peak at about 1150 nm represents the (7,6) chirality nanotubes. Thus the following emission spectra are then analyzed using the intensity of the (7,6) nanotube peak. We define intensity decline rate (f) as: $f\ (\%)=(F_0-F)/F_0$, where F_0 and F represent the intensities of (7,6) nanotube peak before and after Hg^{2+} addition, respectively. The following data analyses are all based on the f value calculation.

To further increase the detection sensitivity and decrease the analyte amount as well as the reaction time, we then conducted the Hg^{2+} triggered NIR fluorescence quenching concept in microfluidic chips system. We mainly compared the following two important reaction conditions and detection performance in Eppendorf tubes and microfluidic chips: (i) volume of reagents; (ii) minimum reaction time to reach the plateau; (iii) detection sensitivity and selectivity. Attributed to the small dimensions of microfluidic chips, the total sample injection quantity was limited to 9 μL, however the sample volume needs about 500 μL in micro quartz cuvette detection. This huge volume decrease not only avoided the large dead volumes of conventional fluidic connectors, but also gave an affirmative solution to the inadequateness of the sample amount in NIR fluorescence test, especially for bioassays with limited small volume of bio-samples. Meanwhile, the occurrence of NIR-on-chip eliminate the anxiety from inadequate collection volume of environment samples in NIR detection, which makes field sample obtaining more convenient than before.

The dynamic process of the mercury triggered SWNTs aggregation was also monitored. Fig. 6 shows the f values changes of d16/SWNTs solutions with the reaction time in microfluidic system (a) and conventional Eppendorf tube system (b) respectively at the same Hg^{2+} concentration. As expected, the minimum reaction time to reach plateau decreased to 30 min in microfluidic chips, only half of 60 min in Eppendorf tubes. We reasoned that comparatively fast reaction time profits from reduced device dimensions, insomuch as the microchannel dimensions are more close to diffusion length and enhanced the diffusion rate of molecules [22]. Therefore, in the following quantitative detection, 30 min and 60 min were set as the reaction time in conventional Eppendorf tube and microfluidic chip system, respectively.

For the quantitative analysis, the NIR fluorescence spectrums of different concentrations of Hg^{2+} containing d16/SWNTs solution from 2.5 nM to 500 nM were investigated in both Eppendorf tubes (Fig. 5) and microfluidic chips system (Fig. 7). Typically, the f values are sensitive to nanomolar final concentrations of Hg^{2+}.

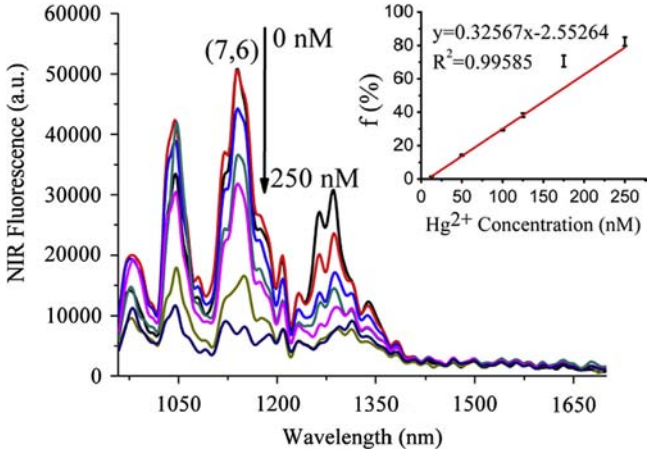

Fig. 5. NIR fluorescence emission spectra of d16/SWNT solution after addition of Hg^{2+} at different concentrations in conventional Eppendorf tubes. The inset shows the linear relationship between the (7,6) nanotube intensity at about 1150 nm and the Hg^{2+} concentration ranging from 12.5 nM to 250 nM.

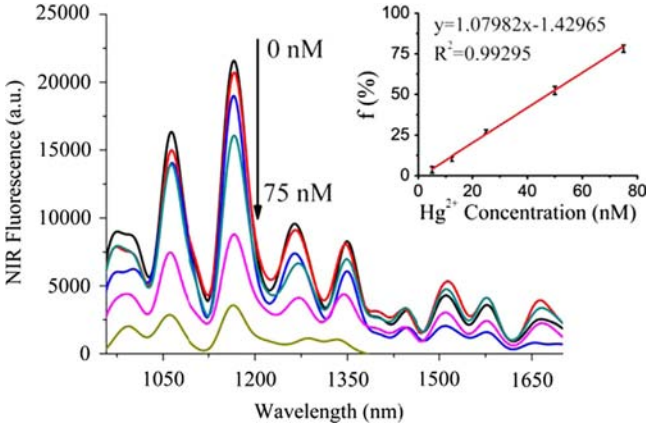

Fig. 7. NIR fluorescence emission spectra of d16/SWNT solution after addition of Hg^{2+} at different concentrations in microfluidic system. The inset shows the linear relationship between the (7,6) nanotube intensity at about 1150 nm and the Hg^{2+} concentration ranging from 5 nM to 75 nM.

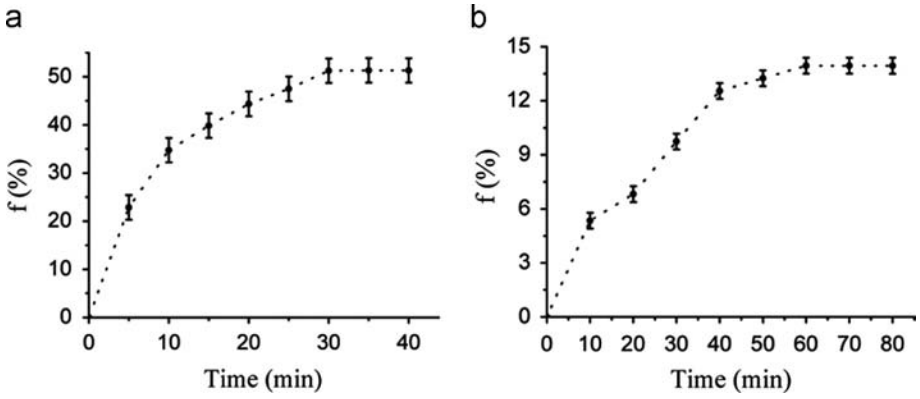

Fig. 6. The minimum reaction time to reach plateau of d16/SWNT solution with concentration of Hg^{2+} at 50 nM (a) in microfluidic system and (b) in Eppendorf tube.

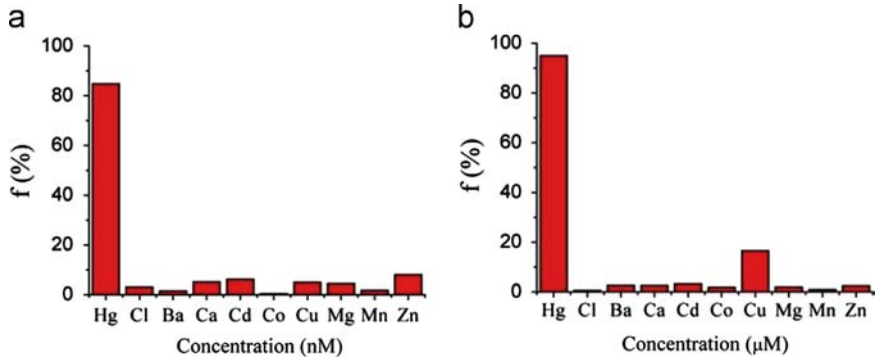

Fig. 8. (a) The difference in f values between d16/SWNT solution containing Hg^{2+} and different other ions in microfluidic system. Concentration of Hg^{2+} is 100 nM and concentrations of Cl^- and other metal ions are both 500 nM. (b) The difference in f values between d16/SWNT solution containing Hg^{2+} and with different other ions in conventional Eppendorf tubes. Concentration of Hg^{2+} is 500 nM and concentrations of Cl^- and other metal ions are both 1 μM.

In Eppendorf tubes, the NIR intensity was not further decreased at Hg^{2+} concentrations of >300 nM since almost all of the dispersed SWNTs which could be detected by NIR fluorescence spectrometer had aggregated as shown in the photograph of Scheme 1(b). The linear relationship range of Hg^{2+} detection in Eppendorf tubes (inset of Fig. 5) is from 12.5 nM to 250 nM ($R^2=0.996$), with the detection limit of 10.5 nM (three times the standard deviation of the blank solution). Meanwhile, in microfluidic chips, the Hg^{2+} detection linear range is from 5 nM to 75 nM ($R^2=0.993$) with the detection limit at 1.5 nM (inset of Fig. 7), which is 7-fold lower than that of tube test system. The decrease of NIR peaks reached to a plateau at Hg^{2+} concentrations of higher than 100 nM in microfluidic chips, and less Hg^{2+} concentration resulted in complete aggregation, which was consistent with the small injection volume. The relatively large specific surface area for reaction of d16/SWNTs shows intrinsic compatibility with the great surface-to-volume ratio offered by microfluidic chips, which could probably improve the collision chances of reactant molecules. We deduce that the above reasons, as well as the reduction of dead volume, both result in the decrease of detection limit. The low detection limit in microfluidic chips is particularly attractive because it is much lower than the guideline value of Hg^{2+} in drinking water set by the World Health Organization (30 nM) and by the US Environmental Protection Agency (10 nM). Therefore, our attempt of NIR-on-chip system not only successfully brings the advantages of microfluidic chip to NIR fluorescence detection field, but also provides sufficient sensitivity below 10 nM in trace Hg^{2+} detection.

To evaluate the selectivity of the microfluidic chips detection system for Hg^{2+}, a series of controlled experiments were carried out. Since Cl^- almost did not contribute in the decline of NIR fluorescence intensity (Fig. 8), the f values of d16/SWNTs solution were tested over the addition of various divalent metal ions, including Ba^{2+}, Ca^{2+}, Cd^{2+}, Co^{2+}, Cu^{2+}, Mg^{2+}, Mn^{2+}, Zn^{2+}. Fig. 8a presents the f values of the d16/SWNT solution after addition of Hg^{2+} (100 nM), or Cl^- (500 nM), or other metal ions (500 nM) in microfluidic systems. Obviously, all the other metal ions affected the d16/SWNTs detection system slightly and could be neglected. Similar results in conventional Eppendorf tubes are shown in Fig. 8b.

3.3. Real environmental water sample analysis in microfluidic chips system

With outstanding sensitivity and selectivity, the microfluidic chips detection system was further evaluated with real environmental water samples. The real environmental samples collected in a nearby river were first filtered through 0.22 μm membrane, then standard Hg^{2+} solution (with known concentration) was added in these samples. Through peristaltic pumps, the real environment samples and d16/SWNTs solution were injected into a microfluidic chip to reach a final Hg^{2+} concentration at 4 nM and 8 nM. After an incubation time of 30 min at room temperature, the NIR fluorescence spectrum was obtained. Comparing to the standard curve above, ratios between measured NIR fluorescence intensity and calculated value achieved to be 0.996 and 1.007 for 4 nM and 8 nM Hg^{2+}, respectively. These results revealed that our system had strong potential in real environment sample detection.

4. Conclusion

In conclusion, we have successfully brought near-infrared fluorescence detection method into microfluidic chip system based on the dissolution and aggregation of label-free ssDNA/SWNTs, which needs neither chemical functionalization of SWNTs nor labeling of ssDNA due to the unique NIR fluorescence of SWNTs. As for Hg^{2+} detection, the NIR-on-chip approach showed significant merits of microfluidic chip systems. Reduced device dimensions of microfluidic chips notably decreased the reagent volume and reaction time, while presented extremely low detection limit at 1.5 nM. The idea of detecting NIR fluorescence spectra in microfluidic systems actually leads to a revolution of traditional NIR fluorescence analysis and would be further transferred to other environmental control and clinical diagnosis.

Acknowledgments

This work is supported by the National Natural Science Foundation of China (20805009, 20890022, 21175029), SRF for ROCS, SEM, Shanghai Leading Academic Discipline Project (B109 & 08XD14010), the Shanghai Nature Science Foundation (12ZR1401700) and the Young Scientist Foundation of Fudan University (08FQ12).

References

[1] A. Star, E. Tu, J. Niemann, J.C.P. Gabriel, C.S. Joiner, C. Valcke, Proc. Natl. Acad. Sci. USA 103 (2006) 921–926.
[2] N.W.S. Kam, M. O'Connell, J.A. Wisdom, H.J. Dai, Proc. Natl. Acad. Sci. USA 102 (2005) 11600–11605.
[3] S.M. Taghdisi, P. Lavaee, M. Ramezani, K. Abnous, Eur. J. Pharm. Biopharm. 77 (2011) 200–206.
[4] M.J. O'Connell, S.M. Bachilo, C.B. Huffman, V.C. Moore, M.S. Strano, E.H. Haroz, K.L. Rialon, P.J. Boul, W.H. Noon, C. Kittrell, J.P. Ma, R.H. Hauge, R.B. Weisman, R.E. Smalley, Science 297 (2002) 593–596.
[5] M. Zheng, A. Jagota, E.D. Semke, B.A. Diner, R.S. McLean, S.R. Lustig, R.E. Richardson, N.G. Tassi, Nat. Mater. 2 (2003) 338–342.
[6] D.A. Heller, E.S. Jeng, T.K. Yeung, B.M. Martinez, A.E. Moll, J.B. Gastala, M.S. Strano, Science 311 (2006) 508–511.

[7] E.S. Jeng, A.E. Moll, A.C. Roy, J.B. Gastala, M.S. Strano, Nano Lett. 6 (2006) 371–375.
[8] H. Chen, C. Yu, C.M. Jiang, S. Zhang, B.H. Liu, J.L. Kong, Chem. Commun. (2009) 5006–5008.
[9] X.E. Fang, H. Chen, S.N. Yu, X.Y. Jiang, J.L. Kong, Anal. Chem. 83 (2011) 690–695.
[10] D. Gallego-Perez, N. Higuita-Castro, S. Sharma, R.K. Reen, A.F. Palmer, K.J. Gooch, L.J. Lee, J.J. Lannutti, D.J. Hansford, Lab Chip 10 (2010) 775–782.
[11] M.S. Aw, J. Addai-Mensah, D. Losic, Chem. Commun. 48 (2012) 3348–3350.
[12] M. Hitzbleck, L. Gervais, E. Delamarche, Lab Chip 11 (2011) 2680–2685.
[13] I. Onyido, A.R. Norris, E. Buncel, Chem. Rev. 104 (2004) 5911–5929.
[14] U.S.E.P. Agency, National Secondary Drinking Water Regulations. The Agency, 1984.
[15] L.B. Zhang, L. Tao, B.L. Li, L. Jing, E.K. Wang, Chem. Commun. 46 (2010) 1476–1478.
[16] S.Y. Niu, Q.Y. Li, R. Ren, K.C. Hu, Anal. Lett. 43 (2010) 2432–2439.
[17] S.J. He, D. Li, C.F. Zhu, S.P. Song, L.H. Wang, Y.T. Long, C.H. Fan, Chem. Commun. (2008) 4885–4887.
[18] D.B. Liu, W.S. Qu, W.W. Chen, W. Zhang, Z. Wang, X.Y. Jiang, Anal. Chem. 82 (2010) 9606–9610.
[19] P.W. Barone, M.S. Strano, Angew. Chem. Int. Ed. 45 (2006) 8138–8141.
[20] J.J. Brege, C. Gallaway, A.R. Barron, J. Phys. Chem. C 111 (2007) 17812–17820.
[21] X.Y. Gao, G.M. Xing, Y.L. Yang, X.L. Shi, R. Liu, W.G. Chu, L. Jing, F. Zhao, C. Ye, H. Yuan, X.H. Fang, C. Wang, Y.L. Zhao, J. Am. Chem. Soc. 130 (2008) 9190–9191.
[22] M.A.M. Gijs, F. Lacharme, U. Lehmann, Chem. Rev. 110 (2010) 1518–1563.